Check for updates

How to cite: *Angew. Chem. Int. Ed.* **2021**, *60*, 23656–23660
International Edition: doi.org/10.1002/anie.202109380
German Edition: doi.org/10.1002/ange.202109380

Helicenes

Zinc-[7]helicenocyanine and Its Discrete π-Stacked Homochiral Dimer

*Fangyuan Zhang, Krzysztof Radacki, Holger Braunschweig, Christoph Lambert, and Prince Ravat**

In memory of Professor Siegfried Hünig

Abstract: *In this communication, we demonstrate a novel approach to prepare a discrete dimer of chiral phthalocyanine (Pc) by exploiting the flexible molecular geometry of helicenes, which enables structural interlocking and strong aggregation tendency of Pcs. Synthesized [7]helicene-Pc hybrid molecular structure, zinc-[7]helicenocyanine (Zn-7HPc), exclusively forms a stable dimeric pair consisting of two homochiral molecules. The dimerization constants were estimated to be as high as* $8.96\times10^{6}\ M^{-1}$ *and* $3.42\times10^{7}\ M^{-1}$ *in THF and DMSO, respectively, indicating remarkable stability of dimer. In addition, Zn-7HPc exhibited chiral self-sorting behavior, which resulted in preferential formation of a homochiral dimer also in the racemic sample. Two phthalocyanine subunits in the dimeric form strongly communicate with each other as revealed by a large comproportionation constant and observation of an IV-CT band for the thermodynamically stable mixed-valence state.*

Phthalocyanines (Pcs) are the closest and most noteworthy synthetic analog of naturally occurring porphyrins.[1] Pcs show an intense absorption band in the NIR region, which renders them to be an excellent light-harvesting system.[2] The remarkable photostability and organic-inorganic hybrid structure of metal Pcs extend their application portfolio to photovoltaics,[3] nonlinear optics, ion sensing,[4] and sensitizers for photodynamic therapy,[5] as well as in catalysis.[6] The introduction of an additional functional element in Pcs, namely chirality, opens up new avenues for their applicability, such as spin-filters,[7] stereoselective catalysis, enantioselective sensing, and quantum-based optical computing.[8] Most common approaches for obtaining chiral Pcs rely on the attachment of chiral solubilizing side chains and decorating peripheral positions with binaphthyl units via ethereal linkages.[9] However, these chiral units are not directly conjugated with the Pc core, which offers limited chirality transfer to the characteristic optical bands of Pc. The chiral Pcs with discrete aggregated structures will advance the understanding of electronic communication in homochiral self-assemblies akin to natural systems. Unfortunately, the strong aggregation tendency of Pcs typically yields insoluble aggregates.[10] An efficient way to create well-defined aggregates is by covalently linking the Pc to a rigid π-spacer, which, however, breaks the symmetry of monomeric units and often results in regioisomers.[11]

Addressing these challenges in obtaining the chiral π-extended Pc with an effective chiroptical response and solution processability, we replaced terminal benzene rings at the corners of perfectly square planar D_{4h}-symmetric Pc with C_2-symmetric configurationally stable [7]helicenes ($\Delta G^{\ddagger}(298\ \mathrm{K}) = 41.2\ \mathrm{kcal\,mol^{-1}}$).[12] The earlier attempt in this direction using [5]helicene suffered from poor configurational stability of helicene units, which yielded a mixture of stereoisomers.[13] Similar work by Katz and co-workers involved the attachment of helicene to an aza-analog of Pc.[14] However, the helicene units were decorated with long alkyl chains, which forbid to realize true impact of three-dimensional structure of helicenes on the solubility and aggregation behavior of Pcs.

Herein we describe the design, stereospecific synthesis, investigation of functional properties, and self-assembly process of a [7]helicene-Pc hybrid molecular structure, namely, zinc-[7]helicenocyanine (Zn-7HPc). During characterization, we discovered that the Zn-7HPc exists as a helically interlocked highly stable homochiral dimer both in solution over a wide concentration range and in the solid state.

Due to four helical substructures and molecular symmetry, Zn-7HPc can exist as six stereoisomers, including two pairs of enantiomers. Considering the large π-conjugated structure of Zn-7HPc, nonstereoselective synthesis would lead to a non-resolvable mixture of stereoisomers. Therefore, taking advantage of the high inversion barrier of [7]helicene, we planned to obtain chiral Zn-7HPc in a stereospecific manner (Scheme 1).[15] The key precursor, enantiopure (*P*)-9,10-dicyano[7]helicene (*P*)-**1**, was synthesized by the reaction of (*P*)-9,10-dibromo[7]helicene with CuCN in a 77% yield (Supporting Information Section S2). The condensation reaction of (*P*)-**1** in the presence of $ZnCl_2$ and DBU in isopentanol yielded optically active (*P*)-Zn-7HPc in 60–70% yield with the retention of configuration. The crystalline (*P*)-Zn-7HPc could be dissolved in coordinating solvents such as

[*] M. Sc. F. Zhang, Prof. C. Lambert, Dr. P. Ravat
Institut für Organische Chemie, Universität Würzburg
Am Hubland, 97074 Würzburg (Germany)
E-mail: princekumar.ravat@uni-wuerzburg.de
Dr. K. Radacki, Prof. H. Braunschweig
Institut für Anorganische Chemie, Universität Würzburg
Am Hubland, 97074 Würzburg (Germany)
Supporting information and the ORCID identification number(s) for the author(s) of this article can be found under: https://doi.org/10.1002/anie.202109380.

© 2021 The Authors. Angewandte Chemie International Edition published by Wiley-VCH GmbH. This is an open access article under the terms of the Creative Commons Attribution Non-Commercial NoDerivs License, which permits use and distribution in any medium, provided the original work is properly cited, the use is non-commercial and no modifications or adaptations are made.

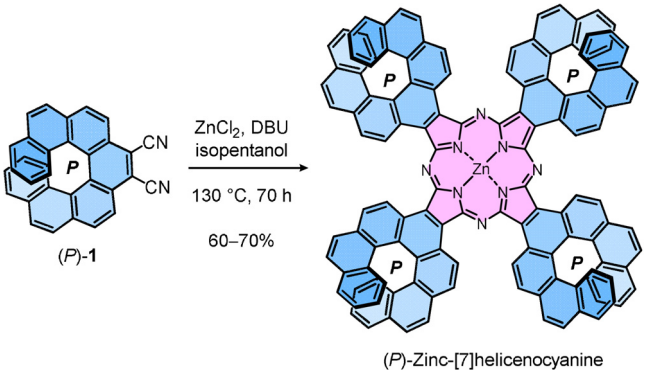

Scheme 1. Stereospecific synthesis of (*P*)-zinc-[7]helicenocyanine.

THF and DMSO. The left-handed congener (*M*)-Zn-7HPc was obtained from corresponding (*M*)-**1**.

The high-resolution MALDI mass spectrometry confirmed the formation of Zn-7HPc (Supporting Information Figure S13). The ^{1}H-NMR spectrum of (*P*)-Zn-7HPc in [D_8]THF ($c \approx 10^{-4}$ M) showed well-resolved resonance signals, which can be assigned to 16 hydrogens of the [7]helicene substructure with the aid of 2D NMR experiments-COSY and NOESY (Figure 1). However, considering the D_4-symmetry of Zn-7HPc, we expected the ^{1}H-NMR spectrum to consist of signals corresponding to only 8 distinct hydrogens. This anomaly was resolved when we obtained the single-crystal structure, which showed that Zn-7HPc exclusively formed a helically-interlocked cofacial dimer in which an axial position of Zn^{II} was occupied by a methanol molecule, the cosolvent of crystallization (Figure 2). The two Zn-7HPc

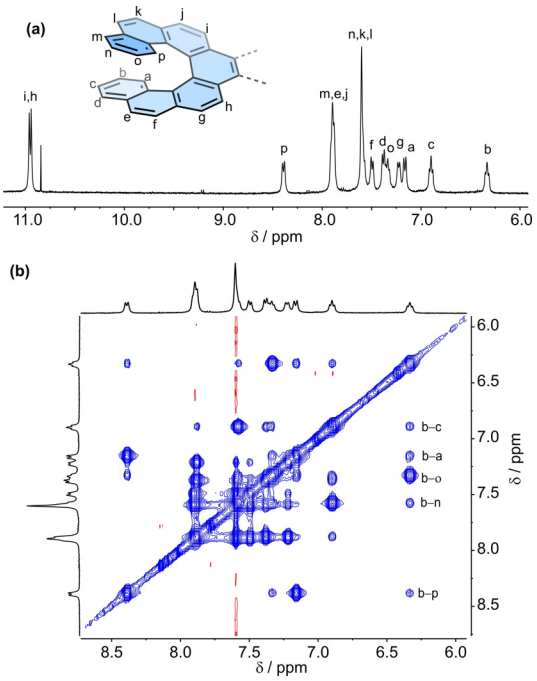

Figure 1. (a) ^{1}H NMR spectrum ($c \approx 10^{-4}$ M) and assigned proton resonance signals using 2D NMR experiments. (b) NOESY spectrum ($c \approx 10^{-4}$ M) showing through space H-H interactions between two molecules.

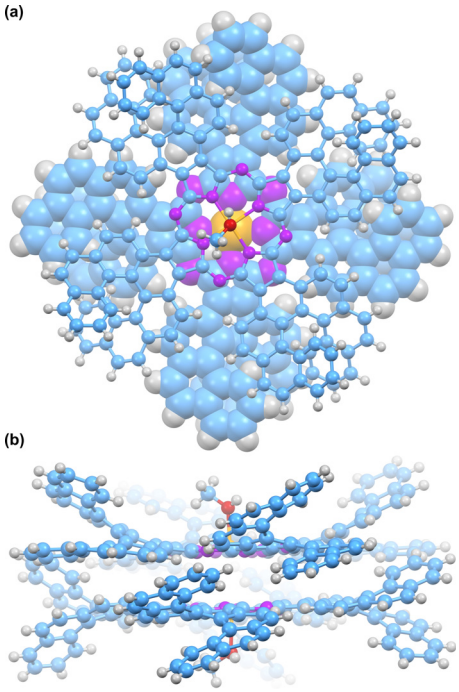

Figure 2. Top and side views (with depth clue) of single-crystal structure of the (*P*)-Zn-7HPc dimer. Color code, H: white, C: blue, N: purple, O: red, Zn: orange.

molecules displayed a staggered arrangement with an interlayer distance of 3.48 Å. It is very likely that Zn-7HPc exist in dimeric form even in the solution, as indicated by the NOESY experiment (Figure 1b). In this cofacial π-stacked dimer, hydrogens of terminal benzene rings of helicene from the upper molecule (H_a, H_b, and H_c) and the lower molecule (H_n, H_o, and H_p) are close enough for dipolar coupling, which reduces symmetry to C_4 (Figure 2b). The DOSY experiments excluded the formation of any higher aggregated structures and showed the presence of unique species in solution with a diffusion coefficient of 4.33×10^{-10} $m^2 s^{-1}$ (Supporting Information Figure S20). Accordingly, the Stokes-Einstein equation provided a calculated hydrodynamic radius of 1.09 nm, which matches with the size of the molecule estimated from the single-crystal structure. Moreover, during the MALDI measurements, a peak corresponding to the dimeric structure was detected (Supporting Information Figure S13). The ratio of the dimer peak increases upon reducing the laser power. Ultimately, at a low laser power, the MALDI plot showed only a dimer peak. This suggests that in the solid-state, the dimeric unit is firmly bound, and high laser power is required to break this structure into two monomeric units.[16] Additionally, the ^{1}H NMR at higher temperatures and titration with pyridine revealed that under such conditions, the dimeric structure couldn't be cleaved into monomers (Supporting Information Figure S25–S29). Therefore, we safely concluded that the Zn-7HPc exists as a stable discrete homochiral dimer in solution and solid-state.

The UV/Vis-NIR absorption spectra of Zn-7HPc in THF and DMSO ($c \approx 10^{-5}$ M) were similar (Figure 3a). The spectrum in THF exhibited characteristic absorption bands related to the Pc structure, a B-band (or Soret band) at

 © 2021 The Authors. Angewandte Chemie International Edition published by Wiley-VCH GmbH

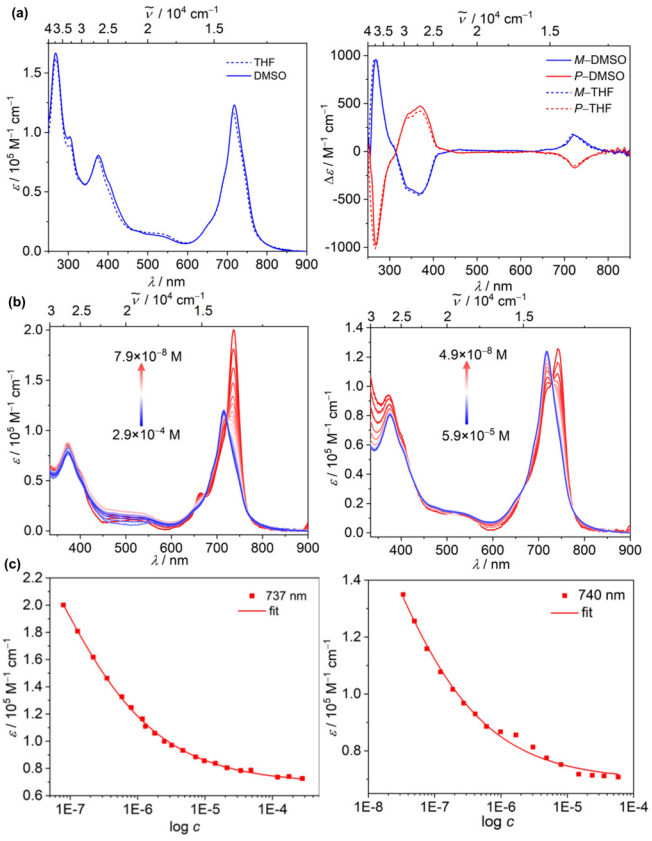

Figure 3. (a) UV/Vis-NIR absorption (left, $c \approx 10^{-5}$ M) and ECD (right, $c \approx 10^{-6}$ M) spectra in THF and DMSO. (b) VC UV/Vis-NIR absorption spectra in THF (left) and DMSO (right) at 298 K. (c) Plot of extinction coefficient (Q-band) against the concentration and global monomer-dimer fit in THF (left) and DMSO (right).

373 nm ($\varepsilon = 78829\ M^{-1}cm^{-1}$) and a Q-band (NIR region) at 715 nm ($\varepsilon = 116445\ M^{-1}cm^{-1}$), both correlate to $\pi \rightarrow \pi^*$ transitions.[17] The relatively high intensity of the B-band, compared to unsubstituted zinc Pc, is likely because of its overlap with the absorption band of [7]helicene.

In order to access the photophysical properties of the monomeric species and to study the aggregation mechanism, we performed variable concentration (VC) UV/Vis-NIR absorption and electronic circular dichroism (ECD) measurements in THF and DMSO. The UV/Vis-NIR investigation of (*P*)-Zn-7HPc in THF revealed that the transition from exclusive dimer to largely monomer occur within the accessible concentration range. As shown in Figure 3b, a significant spectral change was observed by continuously varying the concentration. Zn-7HPc formed a stable dimer in THF up to concentration of 5.0×10^{-6} M, where only a little dissociation could be observed. Upon decreasing the concentration from 5.0×10^{-6} to 7.9×10^{-8} M, a new low energy absorption band at 737 nm with a much higher extinction coefficient appeared, which was assigned to monomeric Zn-7HPc. Apparently, in DMSO, the dissociation is much harder to achieve, and the noticeable spectral changes only occur between the concentration range of 6.0×10^{-7} to 4.9×10^{-8} M indicating a much stronger aggregation than in THF. The hypsochromic and hypochromic shift of the Q-band-because of exciton and vibrational couplings-for dimer confirm the cofacial orientation (H-aggregate) of the molecules following Kasha's molecular exciton theory.[18] When compared with unsubstituted zinc Pc, the monomeric Zn-7HPc showed a large bathochromic shift (928 cm^{-1}) of the Q-band supporting extended π-conjugation.[19] TD-DFT calculations revealed that Zn-7HPc monomer preserves the electronic nature of unsubstituted zinc Pc with the degenerate LUMO and LUMO−1 molecular orbitals. While the Q-band consists of HOMO→LUMO and HOMO→LUMO + 1 transitions with an oscillator strength (*f*) of 0.96, the high energy B-band originates mainly from the HOMO→LUMO + 8 and HOMO→LUMO + 9 transitions with $f = 0.93$ (Supporting Information Table S2).

The aggregation mechanism for supramolecular self-assembly processes can be clarified by fitting the experimental VC UV/Vis-NIR data with different mathematical models.[20] The degree of aggregation lowers with decreasing concentration in both THF and DMSO, which is consistent with supramolecular aggregation under thermodynamic control. The VC UV/Vis-NIR data could be fitted using the monomer-dimer model to yield a dimerization constant $K_{D\,THF} = 8.96 \times 10^6\ M^{-1}$ and $K_{D\,DMSO} = 3.42 \times 10^7\ M^{-1}$ in THF and DMSO, respectively (Figure 3c). Additionally, the observation of well-defined isosbestic points revealed the presence of a thermodynamic equilibrium between monomeric and dimeric Zn-7HPc. $K_{D\,THF}$ and $K_{D\,DMSO}$ are some of the highest reported dimerization constant for the π-π stacked dimeric Pcs.[20] The Zn-7HPc dimer is an unprecedented example of a stable dimeric structure formed exclusively via van der Waals interactions assisted by helical interlocking.[11,21]

The mirror image ECD spectra of (*P*)- and (*M*)-Zn-7HPc in THF and DMSO ($c \approx 10^{-6}$ M, Figure 3a) were also similar. The ECD spectrum of (*M*)-Zn-7HPc in THF displayed three intense CD bands with alternating positive and negative Cotton effects in the UV (265 nm, $|\Delta\varepsilon| = 950\ M^{-1}cm^{-1}$), visible (370 nm, $|\Delta\varepsilon| = 458\ M^{-1}cm^{-1}$), and NIR-region (718 nm, $|\Delta\varepsilon| = 179\ M^{-1}cm^{-1}$). Accordingly, the calculated absorption dissymmetry factors ($g_{abs} = |\Delta\varepsilon|/\varepsilon$) for these three transitions are 0.0058 (265 nm), 0.0059 (370 nm), and 0.0016 (718 nm). The naked [7]helicene shows absorption and CD bands only up to 400 nm.[22] The observation of strong CD effects for electronic transitions associated with Pc core can be attributed to excellent chirality transfer from [7]helicene to Pc following the Kuhn-Kirkwood coupled oscillator and/or the CD stealing mechanism.[9b] The CD spectra of (*M*)-Zn-7HPc in THF at VC, from 4.8×10^{-6} to 9.7×10^{-8} M, displayed a change in CD band only in the NIR region, while the other two bands remained nearly unchanged (Supporting Information Figure S1). The peak maximum at 718 nm from dimer diminished with decreasing the concentration, while the peak at 738 nm from monomer appears, which is in concomitance with VC UV/Vis-NIR absorption spectra.

As our synthetic design provides enantiopure Zn-7HPc, the formation of homochiral self-assembly was evident. However, it was intriguing to verify-if (1) homochirality is necessary to form a stable dimer and (2) the racemic mixture will preferentially compose a heterochiral dimer or other self-assembly. To substantiate this, we prepared a racemic Zn-

 © 2021 The Authors. Angewandte Chemie International Edition published by Wiley-VCH GmbH

7HPc (Supporting Information Section S6). Remarkably, the ^{1}H-NMR spectrum of the racemic mixture in THF was identical to that of homochiral dimer, excluding the formation of heterochiral dimer or any other self-assembled structure (Supporting Information Figure S7). The chiral self-sorting behavior[23] and preferential formation of the homochiral dimer of Zn-7HPc compared to heterodimer is attributed to the interlocked structure between two helicenes of same-handedness assisted by strong aggregation tendency of Pc core as indicated by DFT calculated optimized geometries of homo- and heterochiral dimers (Supporting Information Figure S8). Whereas energies for both type of dimeric structure was similar (the energy difference of only 2.9 kcal mol^{-1}), the heterochiral structure did not exhibit the helical interlocking.

To estimate the electronic coupling among two π-stacked Zn-7HPc units we performed cyclic voltammetry (CV) and differential pulse voltammetry (DPV) as well as spectroelectrochemistry (SEC) experiments in THF ($c \approx 10^{-4}$ M). CV illustrates diffusion-controlled and reversible, one oxidation and two reduction redox couples within the solvent window (Figure 4a). This is in accordance with the typical zinc Pc

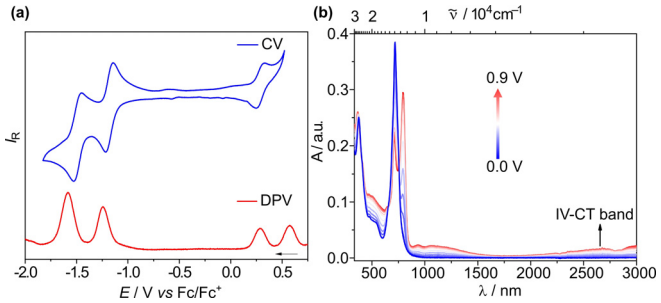

Figure 4. (a) CV (top) and DPV (bottom) voltammograms versus Fc/Fc$^+$ in THF with a supporting electrolyte [Bu$_4$N][PF$_6$] (0.1 M), at a potential sweep rate of 50 mV s^{-1}. (b) SEC data for the first oxidation process.

redox system,[24] but the magnitude of current for the oxidation couple was roughly half that for the each reduction couple. DPV plot provided further evidence for this, as it clearly showed two oxidation waves, at half-wave potentials of 0.28 and 0.58 V, and two reduction waves at −1.24 and −1.58 V with a much higher current. The two oxidation waves can be assigned to one-electron oxidation of the Pc core of each Zn-7HPc (ΔE (Oxi1-Oxi2) = 0.30 V). The oxidation of two chemically identical entities at different potentials indicated that the radical cation of the first oxidized Zn-7HPc in a dimeric structure is stabilized by electronic interaction with second Zn-7HPc molecule. The strong electronic communication within the Zn-7HPc dimer was further supported by the observation of an intervalence charge transfer band (IV-CT band, below 5000 cm^{-1}) upon first oxidation as revealed in SEC experiments (Figure 4b).[25] However, the low intensity of this band exceeding beyond the detection limit (> 3000 nm) of spectrophotometer prevented us from accurately calculating the IV-CT parameters. The comproportionation constant (K_c) values[26] can be considered as an indicator for electronic coupling and thermodynamic stability of the mixed-valence state.[27] Therefore, using the difference of two one-electron oxidation potential values (ΔE), we estimated the $K_c = 1.18 \times 10^5$, which to the best of our knowledge, is one of the highest reported value for discrete π-stacked cofacial Pc dimers.[21,28] Based on the K_c value, the Zn-7HPc dimer was classified as a Robin-Day class II mixed-valence system.

The adequate molecular design and stereospecific synthesis provided an optically active Zn-7HPc in an enantiopure form with good yields and quantities. The synthesized compound exists as a discrete dimer in solution and solid-state. The [7]Helicene units induce an intense CD effect to the characteristic absorption band in the NIR-region of Pc, indicating excellent chirality transfer from peripheral helicenes to Pc core. The VC UV/Vis-NIR absorption spectroscopy, revealed remarkable stability of the homochiral π-stacked dimer and thermodynamic equilibrium between dimer and monomer units in diluted solutions (< 10^{-7} M). Additionally, the Zn-7HPc exhibited chiral self-sorting behavior in the racemic mixture, which shows the importance of homochirality to form a stable self-assembly. Our findings provide insights into electronic communication, stability, and self-assembly mechanism of homochiral Pc dimers. The synthesized optically active Zn-7HPc dimer with a large three-dimensional π-surface will be of potential use in molecular recognition, asymmetric catalysis and as a spin-filter.

Acknowledgements

This project has received funding from the Universität Würzburg within the "Excellent Ideas" program and DFG (Project Number: 448604676). The CPL/CD hybrid spectrometer was funded by the DFG-Project Number: 444286426. We thank Asim Swain and Michael Moos for their help with ECD and SEC measurements. Open Access funding enabled and organized by Projekt DEAL.

Conflict of Interest

The authors declare no conflict of interest.

Keywords: chirality · helicenes · homochiral dimer · phthalocyanines · supramolecular assembly

[1] a) C. G. Bezzu, M. Helliwell, J. E. Warren, D. R. Allan, N. B. McKeown, *Science* **2010**, *327*, 1627–1630; b) P. Gregory, *J. Porphyrins Phthalocyanines* **2000**, *04*, 432–437; c) T. Torres, *J. Porphyrins Phthalocyanines* **2000**, *04*, 325–330.

[2] a) D. Gust, T. A. Moore, A. L. Moore, *Acc. Chem. Res.* **2001**, *34*, 40–48; b) G. Bottari, O. Trukhina, M. Ince, T. Torres, *Coord. Chem. Rev.* **2012**, *256*, 2453–2477.

[3] a) M. Urbani, G. de la Torre, M. K. Nazeeruddin, T. Torres, *Chem. Soc. Rev.* **2019**, *48*, 2738–2766; b) Z. Yu, L. Wang, X. Mu, C.-C. Chen, Y. Wu, J. Cao, Y. Tang, *Angew. Chem. Int. Ed.* **2021**, *60*, 6294–6299; *Angew. Chem.* **2021**, *133*, 6364–6369.

 © 2021 The Authors. Angewandte Chemie International Edition published by Wiley-VCH GmbH

[4] D. Gounden, N. Nombona, W. E. van Zyl, *Coord. Chem. Rev.* **2020**, *420*, 213359.
[5] P.-C. Lo, M. S. Rodríguez-Morgade, R. K. Pandey, D. K. P. Ng, T. Torres, F. Dumoulin, *Chem. Soc. Rev.* **2020**, *49*, 1041 – 1056.
[6] A. B. Sorokin, *Chem. Rev.* **2013**, *113*, 8152 – 8191.
[7] R. Naaman, Y. Paltiel, D. H. Waldeck, *Nat. Rev. Chem.* **2019**, *3*, 250 – 260.
[8] a) H. Lu, N. Kobayashi, *Chem. Rev.* **2016**, *116*, 6184 – 6261; b) Y. Furusho, T. Kimura, Y. Mizuno, T. Aida, *J. Am. Chem. Soc.* **1997**, *119*, 5267 – 5268.
[9] a) M. Á. Revuelta-Maza, T. Torres, G. de la Torre, *Org. Lett.* **2019**, *21*, 8183 – 8186; b) N. Kobayashi, R. Higashi, B. C. Titeca, F. Lamote, A. Ceulemans, *J. Am. Chem. Soc.* **1999**, *121*, 12018 – 12028; c) R. Rai, A. Saxena, A. Ohira, M. Fujiki, *Langmuir* **2005**, *21*, 3957 – 3962.
[10] F. Ghani, J. Kristen, H. Riegler, *J. Chem. Eng. Data* **2012**, *57*, 439 – 449.
[11] N. Kobayashi, *Coord. Chem. Rev.* **2002**, *227*, 129 – 152.
[12] P. Ravat, *Chem. Eur. J.* **2021**, *27*, 3957 – 3967.
[13] B. K. Mandal, T. Sooksimuang, *J. Porphyrins Phthalocyanines* **2002**, *06*, 66 – 72.
[14] J. M. Fox, T. J. Katz, S. Van Elshocht, T. Verbiest, M. Kauranen, A. Persoons, T. Thongpanchang, T. Krauss, L. Brus, *J. Am. Chem. Soc.* **1999**, *121*, 3453 – 3459.
[15] a) F. Zhang, E. Michail, F. Saal, A.-M. Krause, P. Ravat, *Chem. Eur. J.* **2019**, *25*, 16241 – 16245; b) M. Navakouski, H. Zhylitskaya, P. J. Chmielewski, T. Lis, J. Cybińska, M. Stępień, *Angew. Chem. Int. Ed.* **2019**, *58*, 4929 – 4933; *Angew. Chem.* **2019**, *131*, 4983 – 4987.
[16] X.-J. Zhao, H. Hou, X.-T. Fan, Y. Wang, Y.-M. Liu, C. Tang, S.-H. Liu, P.-P. Ding, J. Cheng, D.-H. Lin, C. Wang, Y. Yang, Y.-Z. Tan, *Nat. Commun.* **2019**, *10*, 3057.
[17] "103—Electronic Structures of Metal Phthalocyanine and Porphyrin Complexes from Analysis of the UV/visible Absorption and Magnetic Circular Dichroism Spectra and Molecular Orbital Calculations": J. Mack, M. J. Stillman, in *The Porphyrin Handbook* (Eds.: K. M. Kadish, K. M. Smith, R. Guilard), Academic Press, Amsterdam, **2003**, pp. 43 – 116.
[18] N. J. Hestand, F. C. Spano, *Chem. Rev.* **2018**, *118*, 7069 – 7163.
[19] N. Kobayashi, H. Ogata, N. Nonaka, E. A. Luk′yanets, *Chem. Eur. J.* **2003**, *9*, 5123 – 5134.
[20] Z. Chen, A. Lohr, C. R. Saha-Möller, F. Würthner, *Chem. Soc. Rev.* **2009**, *38*, 564 – 584.
[21] Y. Yamada, K. Nawate, T. Maeno, K. Tanaka, *Chem. Commun.* **2018**, *54*, 8226 – 8228.
[22] Y. Nakai, T. Mori, Y. Inoue, *J. Phys. Chem. A* **2012**, *116*, 7372 – 7385.
[23] F. Helmich, M. M. J. Smulders, C. C. Lee, A. P. H. J. Schenning, E. W. Meijer, *J. Am. Chem. Soc.* **2011**, *133*, 12238 – 12246.
[24] "104—Electrochemistry of Phthalocyanines": M. L′Her, A. Pondaven, in *The Porphyrin Handbook* (Eds.: K. M. Kadish, K. M. Smith, R. Guilard), Academic Press, Amsterdam, **2003**, pp. 117 – 169.
[25] A. Heckmann, C. Lambert, *Angew. Chem. Int. Ed.* **2012**, *51*, 326 – 392; *Angew. Chem.* **2012**, *124*, 334 – 404.
[26] a) R. F. Winter, *Organometallics* **2014**, *33*, 4517 – 4536; b) D. M. D′Alessandro, F. R. Keene, *Dalton Trans.* **2004**, 3950 – 3954.
[27] K_c values obtained from electrochemical measurements depend also on the anion of the electrolyte and solvent. The PF_6^- anion is commonly used in electrochemical measurements involving calculation of K_c values for phthalocyanines and related molecules. A reasonable comparison could be made between the literature and estimated K_c values for Zn-7HPc within the given experimental conditions.
[28] N. Kobayashi, H. Lam, W. A. Nevin, P. Janda, C. C. Leznoff, A. B. P. Lever, *Inorg. Chem.* **1990**, *29*, 3415 – 3425.

Manuscript received: July 14, 2021
Revised manuscript received: August 11, 2021
Accepted manuscript online: August 17, 2021
Version of record online: September 28, 2021

 © 2021 The Authors. Angewandte Chemie International Edition published by Wiley-VCH GmbH